Effect of Reinforcement Corrosion on Axial and Flexural Performance of R.C. Columns

Maha Dabas[1], Beatriz Martin-Pérez[1], Husham Almansour[2]
[1]Department of Civil Engineering, University of Ottawa
800 King Edward, Ottawa, Canada
mdaba091@uottawa.ca; beatriz.martin-perez@uottawa.ca
[2]National Research Council of Canada
1200 Montreal Road, Ottawa, Canada
Husham.Almansour@nrc-cnrc.gc.ca

Abstract – Limited research is available on the axial and flexural performance of statically loaded reinforced concrete columns subject to medium and high levels of corrosion. A combined experimental and analytical investigation was developed to evaluate the residual bearing capacity and the post-peak response of corroded columns at different reinforcement corrosion levels and patterns. The analytical approach was established from sectional analysis and numerical analyses of ten reinforced concrete columns that were experimentally tested under quasi-static concentric and eccentric loads. Eight of the columns were subjected to accelerated reinforcement corrosion for 137-days. The mid-section of the columns was subjected to three different patterns of reinforcement corrosion, targeting the dominating reinforcement contributing to peak bearing capacity depending on eccentricity level. Four columns loaded concentrically and eccentrically were corroded at the transverse reinforcement, two columns loaded eccentrically were corroded along the longitudinal reinforcement only, and two columns loaded concentrically were corroded along the transverse and longitudinal reinforcements. Three-dimensional finite element analyses were conducted using Diana finite element software to investigate more corrosion scenarios beyond those experimentally tested. The presented approach accounts for material deteriorations (strength, cross-sectional area, bond, and confinement effects) using constitutive models from the literature and incorporates data from the experimental testing. The analytical estimation compared well with experimental and numerical results. The outcome of this investigation emphasizes the importance of incorporating degradations models into evaluation procedures of corroded columns. Results indicate a significant reduction in peak residual strength and ductility at high levels of reinforcement corrosion. Also, local buckling of the longitudinal reinforcement is attributed to loss of core confinement due to tie fracture.

Keywords: Reinforcement corrosion, residual strength, post-peak response, experimental and analytical investigation

1. Introduction

Reinforcement corrosion coupled with growth in traffic volume, higher loads, potential inadequate design or improper installation during construction decrease the service life of ageing bridges. Statistics Canada [1] and the Canada Infrastructure Report Card [2] have estimated that 40% of Canadian highway bridges are 80 years old. Moreover, 40% of these bridges have deteriorated and are currently in very/poor to fair condition [2]. Over time, the premature deterioration of reinforced concrete (R.C.) bridges due to reinforcement corrosion leads to concrete cover cracking and spalling/delamination, loss of bond between reinforcement and concrete, and reduction in the structural capacity and ductility of the structure. The Champlain Bridge in Montreal city in Q.C., built in 1962, was recently decommissioned in 2019 due to extensive deterioration of its elements; chloride-induced reinforcement corrosion due to de-icing exposure was one of the main deterioration mechanisms observed [3].

The commentary on the Canadian Highway Bridge Design Code [4-5] addresses the need to develop a detailed quantitative evaluation approach for practicing engineers to assess the condition of deteriorated bridges vulnerable to environmental elements. Evaluation procedures should be conducted according to ULS and SLS to determine a suitable safety level for the bridge [4]. Moreover, it is essential to regularly inspect signs of deterioration visually and to use NDT procedures when necessary [4].

Limited research is available on the structural performance of corroded R.C. columns [6]. The axial behaviour of corroded columns with three different reinforcing details was investigated by Rodriguez et al. [7]. The overall load capacity,

mean strain and compressive stiffness of the R.C. columns were reduced as a result of corrosion of the reinforcement. Wang and Liang [8] and Wang et al. [9] extensive experimental program provides a general insight into the structural response of partially corroded columns exposed to low levels of corrosion. On the other hand, the research of Xia et al. [10] focused on proposing an analytical relationship between the average cross-sectional loss and maximum crack width of the concrete cover.

The effect of reinforcement corrosion and loss of concrete cover on the structural response of R.C. columns was investigated by Tapan and Aboutaha [11-12] using interaction diagrams. Six different cases of reinforcement corrosion patterns with different corrosion levels were investigated for a concrete cover-to-rebar diameter ratio of 1. The authors proposed a modified analytical procedure to calculate interaction diagrams by considering material degradation in concrete and steel due to section and bond loss and damage asymmetry. A bilinear stress-strain curve for corroded reinforcement was used, taking into account the strength reduction of the reinforcement. However, the softening effect of the core of the concrete was not accounted for [10]. Also, a simple analytical model was proposed by Campione et al. [13] to estimate the moment-axial force interaction diagrams for corroded columns. The model considers material deterioration, concrete cover spalling, loss of bond, rebar buckling, and reduction in confinement effects due to tie corrosion. The model accounts for the reduction in confinement effects and potential buckling of the reinforcement. Moreover, a reduction factor is applied to the yielding stress of the longitudinal bar to account for bar slippage due to corrosion. However, corrosion has lesser effects on yield stress and more on the ductility of the longitudinal bars [14].

This paper aims to evaluate the axial and flexural response of corroded columns at different corrosion levels and different corrosion patterns [15]. It examines both the residual strength and post-peak response of the corroded columns. Thus, an experimental program was conducted that involved testing ten columns subjected to concentric and eccentric loadings. Eight of the columns were exposed to different patterns of reinforcement corrosion (ties only, longitudinal bars only, and all the reinforcement cage) after 137-days of an accelerated corrosion regime. The experimental program was extended by conducting three-dimensional nonlinear finite element analyses of corrosion scenarios beyond those tested experimentally. Then a simplified analytical procedure was developed to predict the residual capacity of the corroded columns. The analytical approach estimates the residual load-bearing capacity of corroded columns by considering cover cracking, reduction in confinement effects of the core concrete, potential buckling of the longitudinal bars and bond loss for both concentrically and eccentrically loaded columns.

2. Evaluation of the Axial and Flexural Performance of Corroded Columns

2.1. Experimental Program

A combined experimental and analytical approach was undertaken to predict the residual strength and the post-peak response of the columns. In the experimental program, ten R.C. columns were tested [15]. Five columns were subjected to concentric loads, while the other five were subjected to an eccentric load with an eccentricity of 190 mm. Geometry details are illustrated in Fig. 1. Two columns were control specimens, and the remaining eight were subjected to an accelerated corrosion regime, as shown in Fig. 2. Four cases were tested as follows:

➢ Case 1: Non-corroded, control specimens (C-C-E, C-C-C)
➢ Case 2: Corrosion of the middle two transverse reinforcements (C-C-T1, C-C-T2, C-E-T3, C-E-T4)
➢ Case 3: Corrosion of the longitudinal reinforcement (C-E-R1, C-E-R2)
➢ Case 4: Corrosion of both middle two transverse and longitudinal reinforcement (C-C-All1, C-C-All2).

Ordinary Portland cement concrete ready mix was specified for normal exposure conditions and non-air entrainment. The concrete had a maximum coarse aggregate of 14 mm and a water-to-cement ratio (w/c) of 0.55. The average compressive strength for all columns at 28 days was 33 MPa. For those columns that were subjected to an accelerated corrosion regime, 3.5% of sodium chloride (NaCl) by weight of cement was added to the mixing water to depassivate the protective film on the reinforcement. For the 20M rebars, the yield strength was 446 MPa and the ultimate strain was 0.18. In Table 1, the ultimate load of corroded columns is 55% and 75% of noncorroded columns for concentric and eccentric conditions, respectively. The failure mode of column C-C-All1 was characterized by the widening of pre-existing cracks and spalling, whereas column C-E-T3 had a steel-controlled failure (Fig.3).
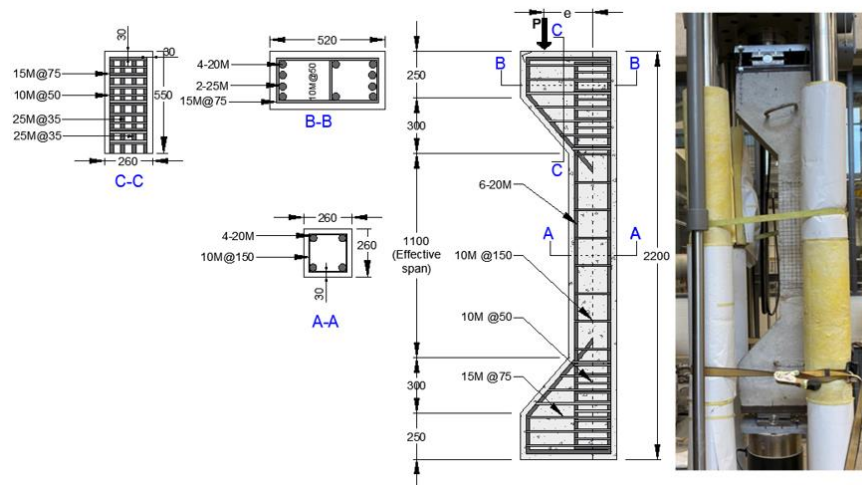
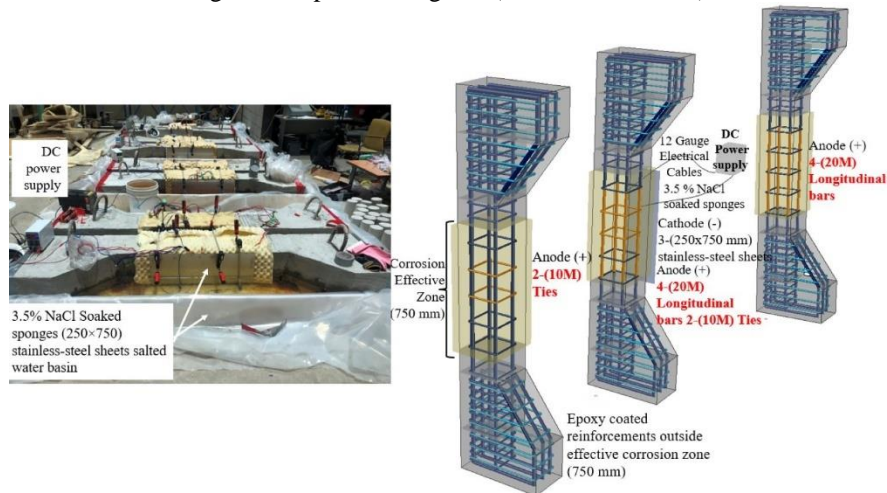Fig. 1:Set-up of loading test (dimensions in mm)
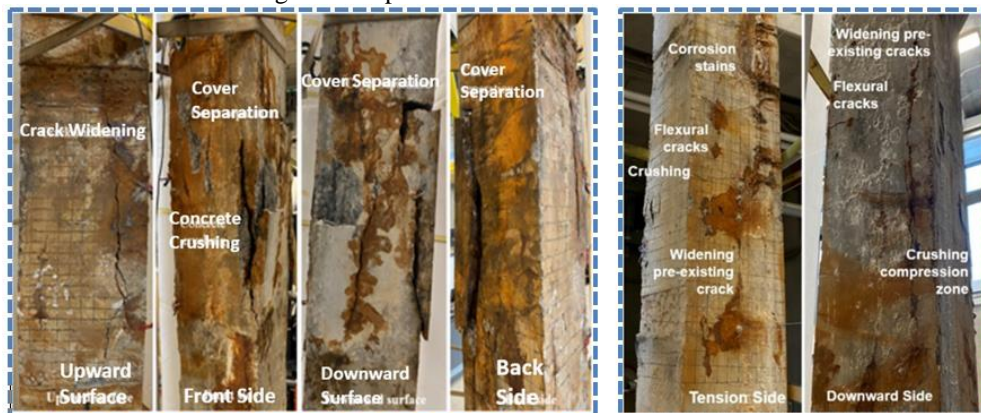

Fig. 2: Set-up of the accelerated corrosion test

Fig. 3: Corrosion damages after load test, Left: concentrically-loaded specimen C-C-All2, Right: Eccentrically-loaded C-E-T3

2.2. Development of a 3D Finite Element Model

A 3D nonlinear finite element analysis (FEA) was developed using Diana software (v.10.5) [16] to analyze further the influence of different corrosion levels on the structural response of columns [15]. In the development of the FEM, the effects of reinforcement corrosion on cracking of the concrete cover, reduction of the cross-sectional area of the reinforcement, and bond loss are accounted for by integrating deterioration models into different sections of the simulated model [15]. Details of the model development and validations are explained in [15]. The numerical models' load-displacement curves capture the failure mode and ultimate displacement as corrosion levels increase (see Fig. 4). The ultimate lateral displacement of corroded columns eccentrically loaded is 60-84% of noncorroded columns, as shown in (Fig. 4). The FEA captures the widespread distribution of flexural cracks and crack width growth (from 2 to 3 mm), as can be seen by comparing the corroded column C-E-R1 to the noncorroded one C-E-C (see Fig. 5).
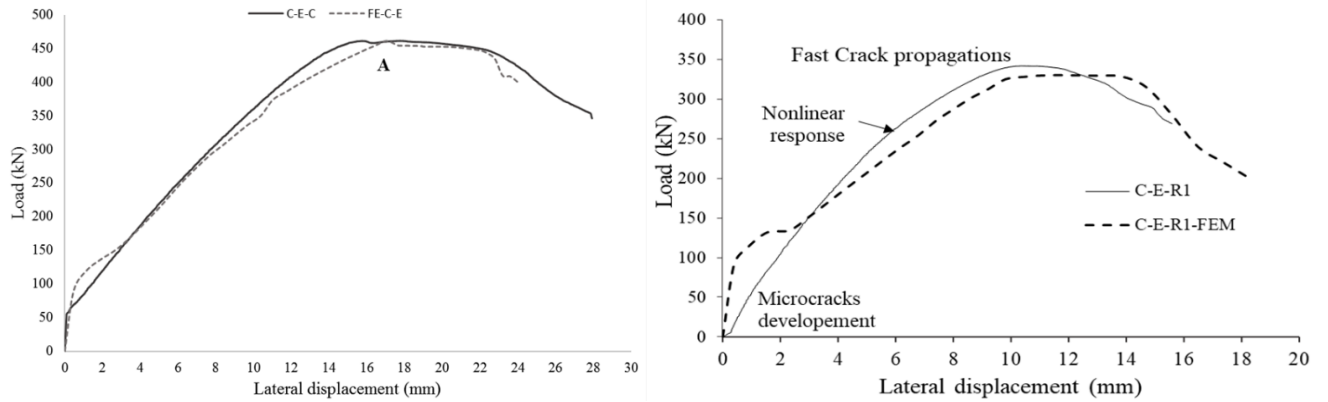

Fig. 4: Validation of the FEM with the experimental results of the control specimen C-E-C and C-E-R1 [15]
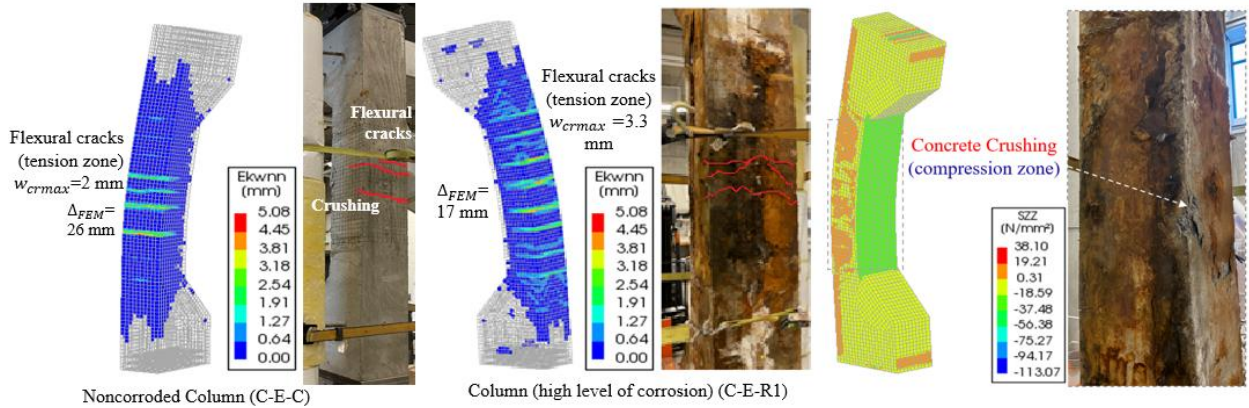

Fig. 5: Crack development: (a) tension zone of C-E-C, (b) tension zone of C-E-R1, (c) compression zone of C-E-R1

2.3. Development of a Simplified Analytical Approach

The residual load capacity for statically loaded columns subjected to reinforcement corrosion (P_c^{corr}) is modified from standard design procedures by incorporating available deteriorating models pertaining to reinforcement corrosion and collected data obtained from field investigations, as follows in Eq. (1):

$$P_c^{corr} = \alpha \cdot \left(f_{cr-cover}(A_{cover}) + f_{core}(A_{core}) \right) + f_y A_{sc} \tag{1}$$

where A_{cover} is the cross-sectional area of the concrete cover, A_{core} is the cross-sectional area of the concrete core, $f_{cr-cover}$ is the reduced compressive strength of the concrete cover, f_{core} is the compressive strength of the concrete core, and f_y and A_{sc} are respectively the yield strength and the cross-sectional area of the corroded reinforcement.

The analytical procedure adopted herein to estimate the residual capacity of corroded columns is detailed as follows and explained in details by Dabas [15]:

- Calculate the reduced area of the concrete cover due to cover cracking according to [15].
- Calculate the position of the neutral axis C_b at the balanced point using strain compatibility. This point is taken as the threshold point between small and large eccentrical loads. Accordingly, the neutral axis position for small and large eccentricity loading conditions can be assumed as C_c and C_e, respectively.
- Determine strain values at the compressive and tensile layers of reinforcement from the strain distribution for large and small load eccentricities, respectively.
- At small loading eccentricities, the compressive bars are assumed to yield, and potential buckling is calculated according to Euler's formulation.
- The compressive steel stress is, then, taken as the minimum of the two values (yielding or buckling). At large eccentricities, the tensile bars are assumed to yield.
- Calculate the reinforcement compressive and tensile F_{s1} and F_{s2} forces for large and small eccentricities, respectively,
- Calculate the maximum bond strength for non-corroded regions τ_{max} according to Rodriguez et al. [17].
- Estimate the residual bond strength τ_{res}.
- Multiply the strain of the tensile bars (eccentric conditions) by a bond reduction factor to account for excessive bar slippage due to corrosion.
- Calculate the tensile force considering steel cross-sectional area reduction and bond loss.
- Calculate the concrete strength C_r incorporating material degradations and geometrical changes as per [15], [18], [19].
- Calculate the residual load capacity according to Eq. (1).
- Calculate the moment capacity and eccentricity (e) from conventional mechanics.

3. Discussion of Results

Table 1 and Fig. 6 illustrate the resulting interaction diagram and the experimental results of specimens C-C-C and C-E-C. Also shown in Fig. 6 are the FEA results corresponding to eccentricities of 0, 40, 100, 130, and 190 mm. The interaction diagram predicts well the capacity of the experimentally-tested and numerically-analyzed columns C-C-C and C-E-C. However, the FEA underestimates the axial capacity at zero eccentricity by 8% (Fig. 6). The experimental results for the corroded columns (C-C-T1, C-C-T2, C-C-All1, C-C-All2, C- E-T3, C-E-T4, C-E-R1 and C-E-R2) are also plotted in Fig. 6. It is evident that the tested corroded columns failed prematurely before reaching the capacity of the control specimen. This indicates that the interaction diagram for non-corroded columns cannot safely predict R.C. columns' axial and flexural capacities affected by reinforcement corrosion. Thus, the analytical approach is established to assess the ultimate capacities of columns subjected to different corrosion levels.

Table 1: Experimental and model validation results

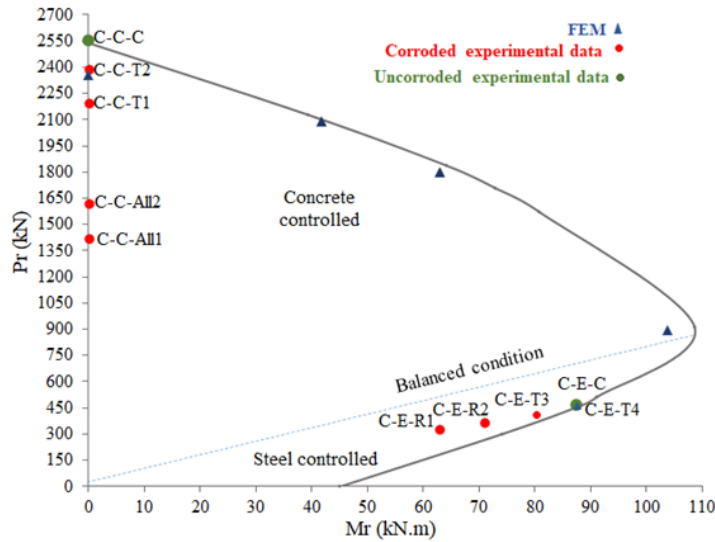| Column	Corrosion level	Average mass loss (%)	$P_{u, Exp}$ (kN)	$P_{u,}$ FEM (kN)	$P_{u,}$ Analytical (kN)	$P_{u,FEM}/P_{u,Exp}$	$P_{u,}$ Analytical $/ P_{u,Exp}$	$P_{u,}$ Analytical $/ P_{u,FEM}$	Rebar-buckle	Tie fracture
C-C-C	None	0	2,550	2,350	2,552	0.92	1.00	1.09	No	No
C-C-T2	Low	3	2,389	2,350	2,352	0.98	0.98	1.00	No	No
C-C-T1	Medium	10	2,199	2,198	2,206	1.00	1.00	1.00	Yes	No
C-C-All2	High	19	1,622	1,622	1,645	1.00	1.01	1.01	No	Yes
C-C-All1	Very high	23	1,418	1,418	1,420	1.00	1.00	1.00	Yes	Yes
C-E-C	None	0	461	461	461	1.00	1.00	1.00	No	No
C-E-T4	Low	4	461	461	461	1.00	1.00	1.00	No	No
C-E-T3	Medium	6	414	435	437	1.05	1.06	1.00	No	No
C-E-R2	Medium	14	369	356	361	0.96	0.98	1.01	No	No
C-E-R1	High	19	342	330	328	0.96	0.96	0.99	No	No
					Mean	0.99	1.00	1.01		
					CV.%	3.40	2.51	2.65		

Fig. 6: Interaction diagram for control column

3.1. Effect of Corrosion of Transverse Reinforcement (Case 2)

The axial and flexural capacities of columns damaged by transverse reinforcement corrosion with an average mass loss ranging from 5% (low) to 20% (very high) are plotted in Fig. 7. Numerical results compared well with the interaction diagrams developed from the sectional analysis. Results indicate that the bearing capacity of the corroded columns is primarily governed by cracking of the concrete cover, reduction in the compressive strength of the concrete core and reduction in confinement effects. Such reduction in confinement was due to a decrease in the lateral pressure on the core concrete, which was reduced by 10% as the tie corrosion level increased by 5%. For high corrosion levels, the spacing between adjacent ties increased due to tie pitting fracture. This assumption is supported by experimental observations from specimens C-C-All1 and C-C-All2. Subsequently, local buckling of the longitudinal bars is observed. Moreover, it is evident that as the level of tie corrosion increases, the reduction in the bearing capacity increases. This reduction is more significant in concrete-controlled columns than steel-controlled columns due to the decrease in concrete confinement provided by the corroded ties.
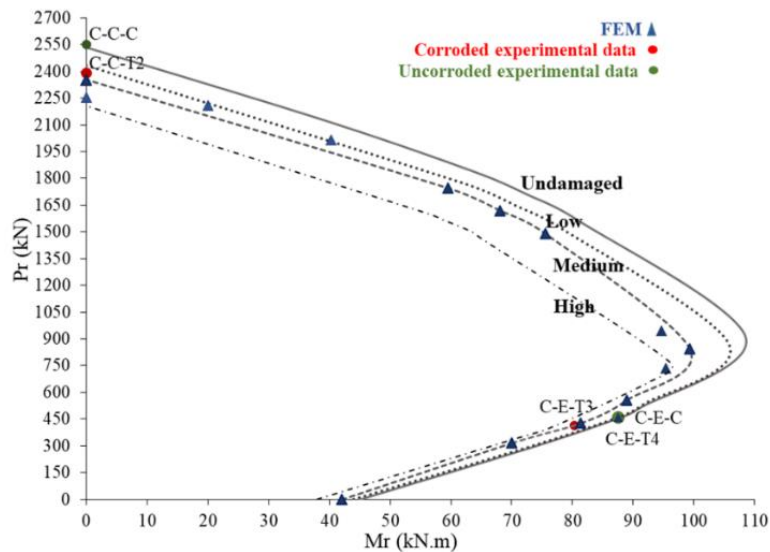

Fig. 7: Interaction diagram for transverse reinforcement (C-C/E-T2) corrosion

ICSECT 117-6

3.2. Effect of Reinforcement Corrosion on Longitudinal Reinforcement (Case 3)

More than a 20% decrement in the axial capacity of R.C columns whose longitudinal reinforcement is corroded to a a medium level when loaded concentrically is illustrated in Fig. 8. For this case, the transverse reinforcement had an average average mass loss of 12%. In case 3, it is found that the ties provided adequate restraining effects to prevent local buckling. buckling.

3.3. Effect of Reinforcement Corrosion on All Reinforcement (Case 4)

A 30-45% reduction in the bearing capacity is illustrated in Fig. 8 for eccentric and concentric loadings, respectively, as the corrosion level is increased for case 4 compared to case 2. This is attributed to significant material deterioration of the reinforcement and concrete (core and cover) and bond loss. For medium to high levels of corrosion, the concrete cover was reduced based on experimental observations of tested columns (C-C-All1, C-C-All2). It was determined that 50% of the concrete cover was still effective in withstanding the applied load. Moreover, local buckling of the longitudinal bars was reported for high levels of corrosion where the corroded ties fractured with a subsequent reduction of the core strength.
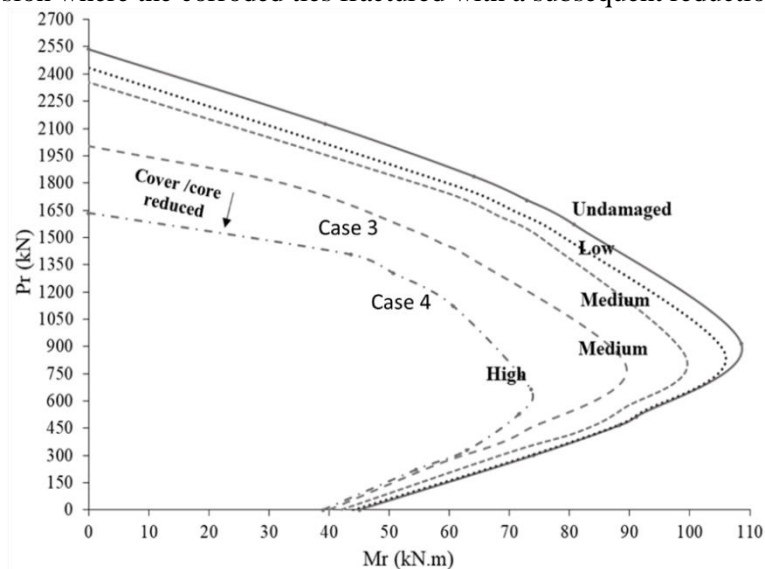
Fig. 8: Interaction diagrams for specimens C-C-C, C-C-ALL, C-E-T, C-E-R

4. Conclusions

Reinforcement corrosion leads to premature material and structural deterioration of R.C. columns, ultimately reducing the overall column's capacity and ductility. Experimental results show that conventional design methods cannot safely predict the ultimate capacity of corroded columns without considering corrosion effects.

An analytical investigation was developed to evaluate the residual capacity and post-peak response of the corroded columns by considering cover cracking, reduction in confinement effects of the core concrete, potential buckling of the longitudinal bars and bond loss at different loading eccentricities. The analytical estimation proposed compared very well with experimental and numerical results for different levels and patterns of reinforcement corrosion. On the other hand, the FEA successfully captured crack distribution, failure mode, and ultimate displacement.

Analytical investigations conclude that the bearing capacity of concrete-controlled columns is significantly affected by the degradations of the concrete cover and loss of confinement. Local buckling of the longitudinal bars was attributed to loss of core confinement due to tie fracture. For eccentrically loaded columns, reduction in residual strength and ductility are significantly affected by reinforcement corrosion and bond loss.

Acknowledgements

References

[1]   Statistics Canada, "Canada's Core Public Infrastructure Survey: Roads, bridges and tunnels, 2016," Canada, 2018. [Online]. Available: https://www150.statcan.gc.ca/n1/en/daily-quotidien/180824/dq180824a-eng.pdf?st=W0rhf8n2.

[2]   Canada Infrastructure Report Card, "Canada Infrastructure Report Card 2019-Monitoring the State of Canada's Core Public Infrastructure," 2019.

[3]   The Jacques Cartier and Champlain Bridges Incorporated (JCCBI)., "Pont Champlain, Services de consultant, Inspections annuelles des sections 5 , 6 et 7 et services d' assistance pour inspections sur demande (2015-2018) – Contrat 62450 Rapport d'inspection 2018 – Volume 1 : Inspection annuelle des sections 5 et 7.," *N/Réf : P-159000038 / M04024D / MTR-00229620*, 2018. https://jacquescartierchamplain.ca/en/the-corporation/reports-and-publications/reports-and-studies/#deconstruction (accessed Mar. 27, 2022).

[4]   CSA-S6.1:19, "Commentary on CSA S6:19, Canadian Highway Bridge Design Code," Canadian Standards Association (CSA Group), Ontario, Canada, 2019.

[5]   CSA Group., *CSA S6:19 Canadian highway bridge design code*, 12th ed. Toronto, Ontario: CSA Group, 2019.

[6]   M. Dabas, B. Martin-Perez, and H. Almansour, "Effects of different patterns of reinforcement corrosion on concrete cover and residual strength in aged bridge piers: state-of-the-art-review," in *Canadian Society of Civil Engineering (CSCE)*, 2021, no. May, pp. 1–10.

[7]   J. Rodriguez, L. M. Ortega, and J. Casal, "Load bearing capacity of concrete columns with corroded reinforcement," in *Corrosion of reinforcement in concrete construction. proceedings of fourth international symposium, Cambridge, 1-4 july 1996. special publication no 183*, 1996, pp. 220–230.

[8]   X. H. Wang and F. Y. Liang, "Performance of RC columns with partial length corrosion," *Nucl. Eng. Des.*, vol. 238, no. 12, pp. 3194–3202, 2008, doi: 10.1016/j.nucengdes.2008.08.007.

[9]   X.-H. Wang, X.-L. Liu, and B.-R. Deng, "Effects of length and location of steel corrosion on the behavior and load capacity of reinforced concrete columns," *J. Shanghai Jiaotong Univ.*, vol. 17, no. 4, pp. 391–400, 2012, doi: 10.1007/s12204-012-1297-6.

[10]   J. Xia, W. Jin, and L. Li, "Performance of corroded reinforced concrete columns under the action of eccentric loads," *J. Mater. Civ. Eng. ASCE*, vol. 28, no. 1, pp. 1–16, 2016, doi: 10.1061/(ASCE)MT.1943-5533.0001352.

[11]   M. Tapan and R. S. Aboutaha, "Strength Evaluation of Deteriorated RC Bridge Columns," *J. Bridg. Eng.*, vol. 13, no. 3, pp. 226–236, 2008, doi: 10.1061/(asce)1084-0702(2008)13:3(226).

[12]   M. Tapan and R. S. Aboutaha, "Effect of steel corrosion and loss of concrete cover on strength of deteriorated RC columns," *Constr. Build. Mater.*, vol. 25, no. 5, pp. 2596–2603, 2011, doi: 10.1016/j.conbuildmat.2010.12.003.

[13]   G. Campione, F. Cannella, L. Cavaleri, and M. F. Ferrotto, "Moment-axial force domain of corroded R.C. columns," *Mater. Struct. Constr.*, vol. 50, no. 1, pp. 1–14, 2017, doi: 10.1617/s11527-016-0930-5.

[14]   J. Cairns, Plizzari.G.A., D. Law, and Franzoni.C., "Mechanical properties of corrosion-damaged reinforcement," *ACI Mater. J.*, vol. 102, no. 4, pp. 256–264, 2005.

[15]   M. Dabas, "Evaluation of the effect of reinforcement corrosion on the structural performance of RC columns." Ph.D. Thesis, Department of Civil Engineering, University of Ottawa, Ottawa,Canada, 2022.

[16]   DIANA FEA BV, "User's Manual -Release 10.5," 2021. https://dianafea.com/manuals/d105/Diana.html (accessed Mar. 22, 2022).

[17]   J. Rodriguez, L. Ortega, and A. Garcia, "Corrosion of reinforcing bars and service life of R/C structures: Corrosion and bond deterioration," in *Proc., Int. Conf. on Concrete across Borders.Vol.II*, 1994, pp. 315–326.

[18]   M. Cape, "Residual service-life assessment of existing R/C structure," Chalmers University of Technology, Goteborg, Sweden and Milan University of Technology Italy, Erasmus Program, 133, 1999.

[19]   M. Razvi, S., and Saatcioglu, "Confinement model for high-strength concrete," *J. Struct. Eng.*, vol. 125, no. 3, pp. 281–289, 1999.